Near-Infrared Colorimetric and Fluorescent Cu²⁺ Sensors Based on Indoline−Benzothiadiazole Derivatives via Formation of Radical Cations

Xumeng Wu,[†] Zhiqian Guo,*[,†] Yongzhen Wu,[†] Shiqin Zhu,[†] Tony D. James,[‡] and Weihong Zhu*[,†]

[†]Shanghai Key Laboratory of Functional Materials Chemistry, Key Laboratory for Advanced Materials and Institute of Fine Chemicals, East China University of Science & Technology, Shanghai 200237, People's Republic of China

[‡]Department of Chemistry, University of Bath, Claverton Down, Bath BA2 7AY, United Kingdom

Ⓢ *Supporting Information*

ABSTRACT: The donor−acceptor system of indoline−benzo-thiadiazole is established as the novel and reactive platform for generating amine radical cations with the interaction of Cu²⁺, which has been successfully exploited as the building block to be highly sensitive and selective near infrared (NIR) colorimetric and fluorescent Cu²⁺ sensors. Upon the addition of Cu²⁺, an instantaneous red shift of absorption spectra as well as the quenched NIR fluorescence of the substrates is observed. The

feasibility and validity of the radical cation generation are confirmed by cyclic voltammetry and electron paramagnetic resonance spectra. Moreover, the introduction of an aldehyde group extends the electron spin density and changes the charge distribution. Our system demonstrates the large scope and diversity in terms of activation mechanism, response time, and property control in the design of Cu²⁺ sensors.

KEYWORDS: *radical cations, donor−acceptor, indoline, near-infrared, copper sensors*
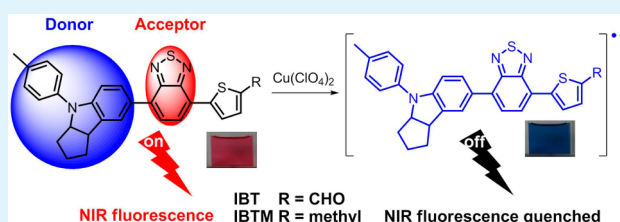
■ INTRODUCTION

Organic radical cations are currently growing attractive concern on their applications in organic magnets, mixed-valence (MV) materials, and biomedicines.[1−10] Particularly, the free radicals can be employed as a probe reporter via monitoring the changes in absorption spectra. For instance, several colorimetric Cu²⁺ sensors have been constructed on the basis of generating the corresponding radical cations via the redox couple Cu²⁺/Cu⁺ in N-containing π-systems.[11,12] However, these systems generally consist of the relatively simple arylamine units with small delocalization π-systems, along with short wavelength fluorescence at around 450 nm.[13−15] To date, novel substrates that feature both near infrared (NIR) fluorescence responses and colorimetric changes via the radical formation are rarely reported.

Copper is an essential nutrient for life and its homeostasis is connected to severe diseases such as Menkes and Wilson diseases and Alzheimer's disease.[16−25] Owing to the biological importance of Cu²⁺, it is greatly desirable to develop NIR colorimetric and fluorescent sensors for Cu²⁺.[26−35] For red-shifting the fluorescence spectra to a longer wavelength, an effective approach is to introduce strong donor and acceptor groups into π-conjugated chromophores. Inspired by the successful strategy of organic sensitizers used in dye-sensitized solar cells (DSSCs), the strong donor−acceptor (D−A) system of indoline−benzothiadiazole, which exhibits promising performance in DSSCs, is employed as an active building block to construct two novel derivatives, **IBT** and **IBTM** (Scheme

1),[36−41] with several meritorious features: (i) utilizing the strong electron-donor indoline unit instead of triphenylamine

Scheme 1. Chemical Structures of IBT and IBTM on the Platform of D−A System
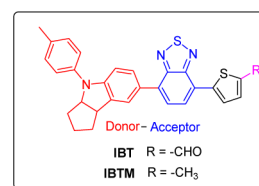
as the reactive platform for generating amine radical cations; (ii) exhibiting NIR fluorescence from the intramolecular charge transfer (ICT) process in a strong D−A system, which can be altered by the Cu²⁺-induced radical cation formation; (iii) endowing better stability of corresponding radical cations via extending spin density and changing charge distribution upon attachment with aldehyde unit in **IBT**. Accordingly, **IBT** becomes a more qualified selective NIR colorimetric and fluorescent Cu²⁺ sensor than **IBTM**. To the best of our knowledge, the novel building block of indoline−benzothiadia-zole is the first reactive NIR fluorescence platform for

generating amine radical cations. Additionally, we focused on the feasibility of the novel indoline−benzothiadiazole platform to generate radical cations and the influence of molecular structure on radical cation stability. Our system demonstrates the large scope and diversity in terms of activation mechanism, response time, and property control in the design of Cu^{2+} sensors.

■ RESULTS AND DISCUSSION

IBT and **IBTM** were obtained easily with high yield by two steps (Scheme S1 in the Supporting Information).[37] Their absorption and fluorescence properties were studied in CH_3CN. For instance, **IBT** exhibits a broad absorption band at 512 nm (ε = 17 600 M^{-1} cm^{-1}) in the visible region, which stems from the ICT process (Figure 1). With addition of
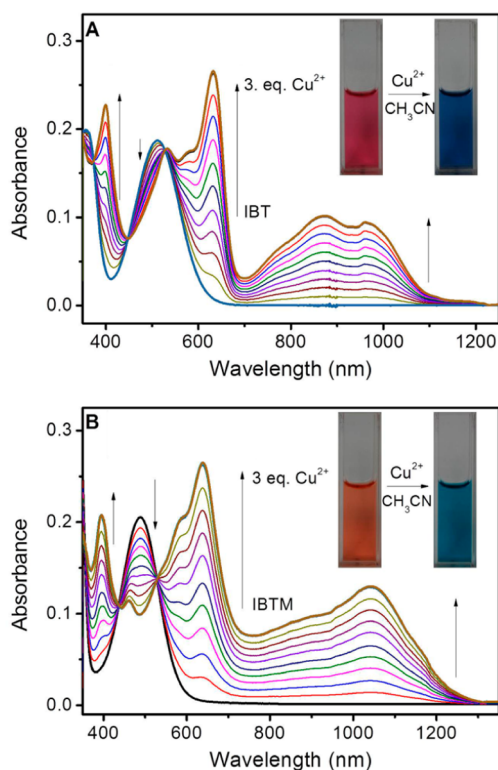

Figure 1. Absorption spectra of (A) **IBT** and (B) **IBTM** (10 μM) upon the titration of $Cu(ClO_4)_2$ (0−3 equiv) in CH_3CN. (Inset) color changes upon addition of $Cu(ClO_4)_2$. Each spectrum was recorded immediately after the addition of $Cu(ClO_4)_2$.

$Cu(ClO_4)_2$, new absorbance peaks in the visible and NIR regions of **IBT** at 400, 532, 633, 872, and 959 nm (ε = 26 300 M^{-1} cm^{-1} for 633 nm) gradually appear (396, 646, and 1042 nm for **IBTM**) with a concomitant decrease of the ICT band at 512 nm (490 nm for **IBTM**). The well-defined isosbestic points at 375, 445, and 529 nm (437 and 529 nm for **IBTM**) can be clearly observed. Moreover, the absorbance ratio A_{633nm}/A_{512nm} of **IBT** increases linearly with the addition of 0−1.0 equiv of Cu^{2+}, which indicates a 1:1 stoichiometry of **IBT** with Cu^{2+} (Figure 2). Meanwhile, the extremely rapid and distinct color change from red violet to blue can also be observed by naked eyes (insets of Figure 1). The significant NIR absorption of **IBT** and **IBTM** after Cu^{2+} addition can be attributed to the generation of corresponding radical cations.
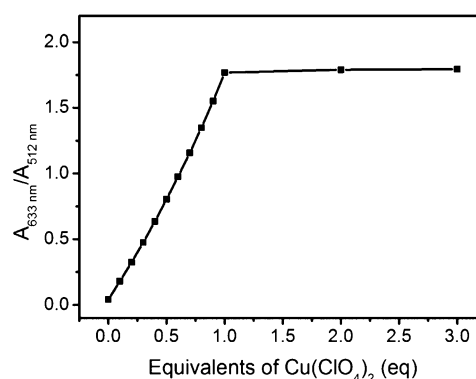

Figure 2. Ratiometric calibration curve A_{633nm}/A_{512nm} for **IBT** as a function of equivalent of $Cu(ClO_4)_2$.

Remarkably, the fluorescence bands of both **IBT** and **IBTM** are located at 750 and 720 nm (Figures 3A and S1A in the

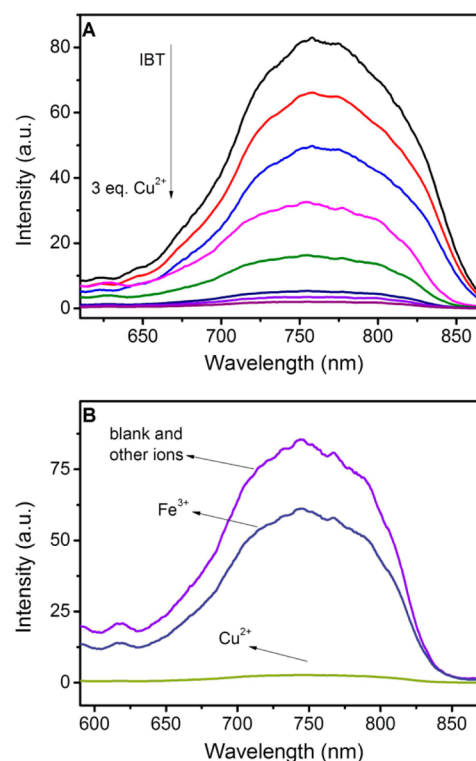**Figure 3.** Fluorescence spectra of **IBT** (10 μM) in CH_3CN: (A) titration of 0−3 of equiv Cu^{2+}; (B) addition of 5 equiv of various metal ions (Co^{2+}, Ca^{2+}, Ag^+, Mn^{2+}, Pb^{2+}, Na^+, Mg^{2+}, Cd^{2+}, Zn^{2+}, Fe^{2+}, Ni^{2+}, K^+, Fe^{3+}, Cu^{2+}, Cr^{3+}, Sn^{2+}, and Hg^{2+}). The excitation wavelength is 529 nm from the isosbestic point.

Supporting Information), respectively, falling into the NIR region due to the strong ICT process in the D−A system of indoline−benzothiadiazole. Upon titration of Cu^{2+}, their fluorescence becomes almost quenched (Figures 3A and S1A in the Supporting Information), which is consistent with the previously radical cation based Cu^{2+} sensors with high selectivity.[11−15] The detection limit of **IBT** to Cu^{2+} was calculated to be 1.03 × 10^{-6} M in CH_3CN (Figure S1B in the Supporting Information). Here the observed quenching in fluorescence can be rationalized by the resulting unpaired electron from the radical cations (**IBT**$^{+\bullet}$ and **IBTM**$^{+\bullet}$) with

12216

dx.doi.org/10.1021/am404491f | ACS Appl. Mater. Interfaces 2013, 5, 12215−12220

interaction of Cu^{2+}. As a matter of fact, the alterations in absorption and fluorescence spectra can be completely recovered by electron donor such as triethylamine (Figure S2 in the Supporting Information). Moreover, the redox properties of **IBT** and **IBTM** were investigated in CH_3CN by cyclic voltammetry (CV, Figure S3 in the Supporting Information). The first oxidation potential of **IBT** was +0.743 V (**IBTM** for +0.699 V) vs SCE in CH_3CN (Table 1). The free energy

Table 1. Oxidation and Redox Potentials, Calculated Free Energy, and Experimental HOMO Levels

compound	E^1_{ox} (V)	E^1_{redox} (V)	ΔG_{ET} (eV)	HOMO $(eV)^a$
IBT	+0.743/+0.673	0.708	−0.208	−5.143
IBTM	+0.699/+0.632	0.665	−0.252	−5.009
$Cu(ClO_4)_2$	+1.044/+0.858	0.951		

^{a}HOMO level was calculated using following equation: $E_{HOMO} = -(4.4 + E^1_{ox})$ eV.

change was calculated from the Rehm−Weller equation $\Delta G^0 = E_{ox} - E_{red} - e^2/d\varepsilon$, where E_{ox} is the first oxidation potential of the electron donor (**IBT** and **IBTM** in this case), E_{red} is the redox potential of the electron acceptor (Cu^{2+} in this case), d is the center-to-center distance between the donor and acceptor in the collision, and ε is the dielectric constant of CH_3CN (37). In polar solvents like acetonitrile, the Coulombic term is neglected. Their free energy change (ΔG_{ET}) in the exergonic thermal electron transfer from **IBT** and **IBTM** to Cu^{2+} is −0.208 and −0.252 eV, respectively.[42] Obviously, the formation of **IBT$^{+\bullet}$** and **IBTM$^{+\bullet}$** are thermodynamically feasible in CH_3CN.

Electron paramagnetic resonance (EPR) spectroscopy is a powerful approach to detect free radicals or inorganic complexes in chemical and biological systems. Upon titration of 0.5 equiv of Cu^{2+}, a unique EPR peak at $g = 2.0019$ with a peak-to-peak width of 10 G was observed in the EPR spectra of **IBT** (Figure 4), whereas the broad peak for paramagnetic Cu^{2+}
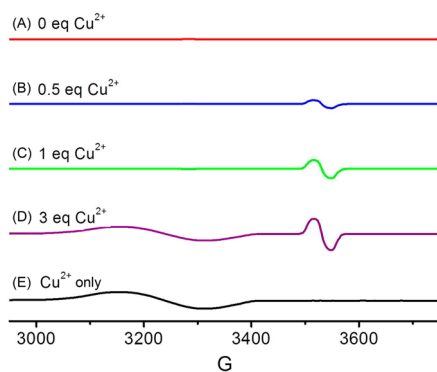

Figure 4. EPR spectra of $Cu(ClO_4)_2$ (10 mM) in CH_3CN and **IBT** (5 × 10^{-4} M) with different equivalents of Cu^{2+} at 298 K. Note: curve E is the EPR signal of the solution of $Cu(ClO_4)_2$ (10 mM) in CH_3CN as a control experiment.

was not found. This unique peak can be attributed to the formation of **IBT$^{+\bullet}$** in concomitance with a reduction of Cu^{2+} to Cu^+. However, adding excess Cu^{2+} to **IBT**, there exhibited both a typical broad EPR peak of Cu^{2+} and the unique signal of **IBT$^{+\bullet}$** (for **IBTM** in Figure S4 in the Supporting Information). Undoubtedly, the radical cations of **IBT$^{+\bullet}$** and **IBTM$^{+\bullet}$** are

formed upon oxidation of **IBT** and **IBTM** in concomitance with a reduction of Cu^{2+} to Cu^+.

Radical cations are generally subvalent compounds with high reactivity and transient nature, which is not preferable for chemosensors. Therefore, the stability of the organic radical cations **IBT$^{+\bullet}$** and **IBTM$^{+\bullet}$** was further studied by the time-dependent absorption analysis. An extremely sharp increase in the resulting absorption bands was observed for **IBT** and **IBTM** (Figure S5 in the Supporting Information), indicative of the fairly high response rate via generating the corresponding radical cations. The absorbance of **IBT** at 633 nm reached a plateau, keeping the same value with almost no decrease in 10 min (Figure 5A). In contrast, the absorbance of **IBTM** at 646
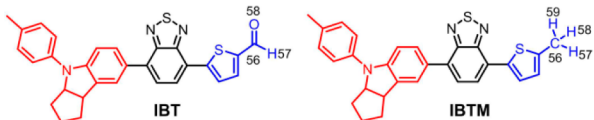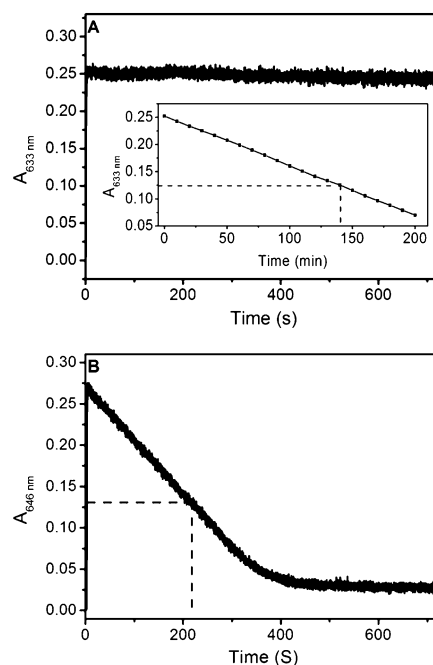

Figure 5. Time course of the absorbance in CH_3CN (10 μM) after the addition of 5 equiv of Cu^{2+}: (A) **IBT** (monitored at 633 nm) and (B) **IBTM** (monitored at 646 nm). Data was recorded every 0.5 s. Inset of A: the time dependence on the absorbance at 633 nm of **IBT** in a larger time range.

nm decreased very quickly, falling down to only 10% of the maximum value within only 7 min (Figure 5B). As a matter of fact, the half-life time of **IBT$^{+\bullet}$** (8400 s) is 35-fold longer than that of **IBTM$^{+\bullet}$** (220 s) in CH_3CN solution. Clearly, **IBT$^{+\bullet}$** has much better stability than **IBTM$^{+\bullet}$**, making **IBT** a more preferable candidate as a NIR Cu^{2+} sensor.

To get further insight into the relationship of stability and molecular structure between the radical cations of **IBT$^{+\bullet}$** and **IBTM$^{+\bullet}$**, the spin density distribution and natural charge were performed by density functional theory (DFT) and time-dependent DFT calculations at the B3LYP/6-31+G(d,p) level of theory.[43] In both **IBT$^{+\bullet}$** and **IBTM$^{+\bullet}$**, the nitrogen atom (N24 in Tables S1 and S2 in the Supporting Information) on the indoline unit possesses the maximum spin density followed by the skeleton carbons. It is worth noting that the atoms on the aldehyde unit (C56, H57, and O58 in Table S1 in the Supporting Information) in **IBT$^{+\bullet}$** participate in the spin density to a much larger extent than that of methyl group (C56, H57−59 in Table S2 in the Supporting Information) in **IBTM$^{+\bullet}$**. This can be attributed to the formation of the specific

12217

dx.doi.org/10.1021/am404491f | ACS Appl. Mater. Interfaces 2013, 5, 12215−12220

conjugation between thiophene and carbonyl groups (Table 2). All these results are in good agreement with the resonance

Table 2. Spin Density of the Aldehyde Group (IBT$^{+\bullet}$) and the Methyl Group (IBTM$^{+\bullet}$) and Partial Charges of IBT$^{+\bullet}$ and IBTM$^{+\bullet}$ Calculated at the B3LYP/6-31+G(d,p) Level

IBT$^{+\bullet}$			IBTM$^{+\bullet}$		
atom no.	atom label	spin density	atom no.	atom label	spin density
56	C	−0.01029	56	C	−0.00454
57	H	−7 × 10^{-5}	57	H	0.0057
58	O	0.03221	58	H	0.00569
			59	H	0.00014
partial charge					
indoline unit	BTD^{a} unit	thiophene unit	indoline unit	BTD unit	thiophene unit
+0.756	+0.098	+0.146	+0.663	+0.078	+0.259

^{a}BTD means benzothiadiazole.

structures of **IBT$^{+\bullet}$** and **IBTM$^{+\bullet}$**. More extension in the spin density distribution by the aldehyde group was observed in their resonance structures (Figures S6 and S7 in the Supporting Information). Moreover, the charge distribution of **IBT$^{+\bullet}$** and **IBTM$^{+\bullet}$** also indicates that the indoline unit of **IBT$^{+\bullet}$** bears more positive charge than that of **IBTM$^{+\bullet}$** (Table 2). As a consequence, the introduction of an aldehyde group to **IBT** can gather the positive charge in the electron-rich indoline unit, resulting in the delocalization of the unpaired electron and the positive charge redistribution to enhance the stability of its radical cation **IBT$^{+\bullet}$**.

Considering the remarkable response to Cu^{2+} and better stability, **IBT** exhibits great potential applications as NIR colorimetric and fluorescent Cu^{2+} sensors. Therefore, the solvent and ion selectivity of **IBT** were also evaluated. Among common solvents, the distinct generation of indoline radical cations can only be observed in CH$_3$CN, possibly arising from the formation of the stable tetra(acetonitrile) copper(I) complex ([Cu(CH$_3$CN)$_4$]$^+$) immediately following the electron transfer (Figure S8 in the Supporting Information).[44] Actually, this may also be part of the driving force for the reaction between **IBT** and Cu(ClO$_4$)$_2$ in CH$_3$CN.[8] Then, the selectivity of **IBT** to Cu^{2+} was also studied in CH$_3$CN with other metal ions. Among the various test metal ions, only Cu^{2+} with **IBT** displayed significant changes in both absorption and emission spectra (Figures 3B and 6). However, the slight interference of Fe^{3+} in fluorescence (Figure 3B) can be neglected because there is no change in the absorption spectra. Additionally, as demonstrated by the further competing experiment, the existence of other ions, even Fe^{3+}, has ignorable interference to the response ability of **IBT** to Cu^{2+} (Figure S9 in the Supporting Information), indicative of the high selectivity of **IBT** to Cu^{2+} with an excellent capacity of resisting disturbance.

■ CONCLUSIONS

The D−A system of indoline−benzothiadiazole as a building block was designed as NIR colorimetric and fluorescent Cu^{2+}
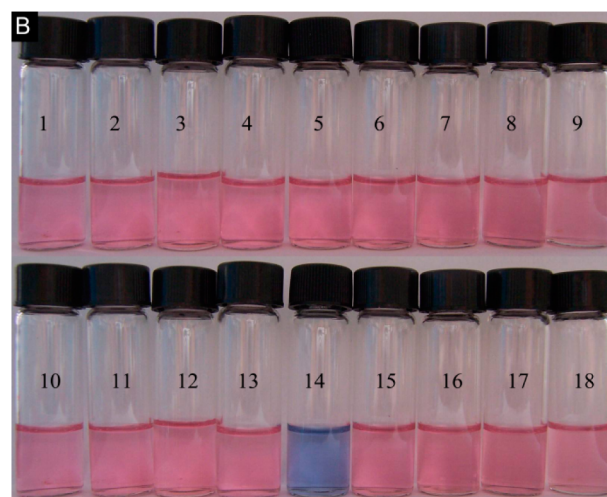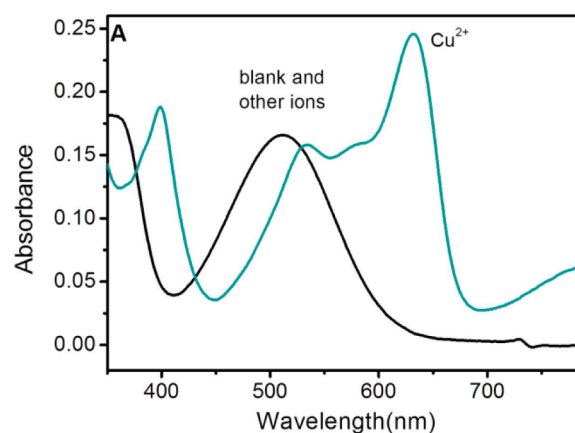

Figure 6. (A) Absorption spectra of **IBT** (10 μM) and (B) colorimetric changes of **IBT** upon addition of 5 equiv of various metal ions in CH$_3$CN: 1, Co^{2+}; 2, Ca^{2+}; 3, Ag$^+$; 4, Mn^{2+}; 5, Pb^{2+}; 6, Na$^+$; 7, Mg^{2+}; 8, Cd^{2+}; 9, Zn^{2+}; 10, Fe^{2+}; 11, Ni^{2+}; 12, K$^+$; 13, Fe^{3+}; 14, Cu^{2+}; 15, Cr^{3+}; 16, Sn^{2+}; 17, Hg^{2+}; 18, IBT only.

sensors via unique radical formation. The ability of **IBT** and **IBTM** to generate corresponding radical cations with the interaction of Cu^{2+} was demonstrated by CV measurement and EPR spectra. Importantly, introduction of the aldehyde unit in **IBT** endows **IBT$^{+\bullet}$** with much better stability than **IBTM$^{+\bullet}$** by extending spin density and changing the charge distribution. The highly selective color change from red to blue with distinct NIR fluorescence response in 750 nm can be specifically developed as long wavelength Cu^{2+} sensors. We believe that this novel platform can provide a new strategy to design NIR colorimetric and fluorescent Cu^{2+} sensors via radical reaction.

■ EXPERIMENTAL SECTION

Materials and Characterization. The starting materials of 4,7-dibromobenzo[1,2,5]thiadiazole (BTD), 7-bromo-1,2,3,3a,4,8b-hexahydro-4-(4-methylphenyl)cyclopent-[b]indole (IN) in Scheme S1 in the Supporting Information were synthesized according to the reference.[41] THF was dried over 4 Å molecular sieves and distilled under argon atmosphere from sodium benzophenone prior to use. All other solvents and chemicals were purchased commercially, and used as received without further purification. ^{1}H and ^{13}C NMR in DMSO-d_6 were recorded on a Bruker AvanceIII 400 MHz instrument with tetramethylsilane (TMS) as the internal standard. Data for ^{1}H NMR spectra was reported as follows: chemical shift (ppm) and multiplicity (s = singlet, d = doublet, t = triplet, q = quartet, m = multiplet). Data for ^{13}C NMR spectra is reported in ppm. HRMS was performed using

a Waters LCT Premier XE spectrometer. Electron paramagnetic resonance (EPR) spectra were recorded using a Bruker EMX-8/2.7C EPR spectrometer. UV−vis-NIR spectra were measured with a Varian Cary 500 spectrophotometer (1 cm quartz cell). Emission spectra were measured with Varian Cary Eclipse (1 cm quartz cell). Flash chromatography was conducted by using silica-gel column packages purchased from Qingdao Haiyang Chemical Co. Absorption changes (stability) were monitored by a CCD camera mounted on a spectrometer (Ocean optics). The absorption spectra of **IBT** and **IBTM** were measured at 25 °C in acetonitrile solution. Stock solution (0.01 M) of the perchlorate salts of Co^{2+}, Ca^{2+}, Ag^+, Mn^{2+}, Pb^{2+}, Na^+, Mg^{2+}, Cd^{2+}, Zn^{2+}, Ni^{2+}, K^+, Fe^{3+}, Cu^{2+}, Cr^{3+}, Hg^{2+}, sulfate salt of Fe^{2+}, and the hydrochloride salt of Sn^{2+} were prepared in CH_3CN, respectively.

Electrochemistry. The electrochemical properties were studied using a computer-controlled Versastat II electrochemical workstation (Princeton Applied Research) using a three-electrode cell with a Pt working electrode, a Pt wire auxiliary electrode, and a saturated calomel reference electrode in saturated KCl solution. 0.1 M tetrabutylammonium hexafluorophosphate ($TBAPF_6$) was used as the supporting electrolyte in CH_3CN. The scan rate for cyclic voltammetry (CV) experiments was typically 100 mV/s.

Synthesis of IB. To a solution of **IN** (2.0 g, 6.1 mmol) in dry THF (30 mL) was injected n-BuLi (3.6 mL, 9.0 mmol) dropwise at −78 °C under argon in the dark. After the solution was stirred for 30 min at −78 °C, $B(OCH_3)_3$ (1.0 mL, 9.0 mmol) was injected. The reaction mixture was stirred at the same temperature for 4 h and then gradually warmed up to room temperature and used for the next Suzuki coupling reaction without purification. The unpurified mixture was reacted with **BTD** (1.8 g, 6.1 mmol) under Suzuki coupling reaction using a $Pd(PPh_3)_4$ (0.58 g, 0.5 mmol) and K_2CO_3 aqueous solution (10 mL, 2 M) as a catalyst in THF (30 mL) for 12 h. After the solution cooled, water was added and the reaction mixture was extracted with CH_2Cl_2. The combined organic layer was washed with H_2O and brine, dried over anhydrous Na_2SO_4, and evaporated under vacuum. The crude product was purified by column chromatography (CH_2Cl_2/petroleum ether = 1/10) on silica gel, and the single substituted product was obtained as a red solid **IB** (1.0 g, 2.1 mmol, 35.5% for two steps). Melting point: 145.3−148.8 °C. ^{1}H NMR (400 MHz, $CDCl_3$, ppm): δ 7.85 (d, J = 7.7 Hz, 1H, Ph-H), 7.70 (s, 1H, Ph-H), 7.64 (dd, J_1 = 8.3 Hz, J_2 = 1.8 Hz, 1H, Ph-H), 7.50 (d, J = 7.6 Hz, 1H, Ph-H), 7.23 (d, J = 8.5 Hz, 2H, Ph-H), 7.17 (d, J = 8.4 Hz, 2H, Ph-H), 6.99 (d, J = 8.3 Hz, 1H, Ph-H), 4.89−4.82 (m, 1H, N−CH−CH), 3.96−3.88 (m, 1H, N−CH−CH), 2.34 (s, 3H, −CH₃), 2.14−2.03 (m, 1H, indoline-H), 1.99−1.89 (m, 2H, indoline-H), 1.86−1.75 (m, 1H, indoline-H), 1.73−1.59 (m, 2H, indoline-H). ^{13}C NMR (100 MHz, $CDCl_3$, ppm): δ 153.99, 153.37, 148.77, 140.01, 135.44, 134.49, 132.47, 131.88, 129.84, 128.87, 126.37, 126.34, 125.50, 120.45, 110.88, 107.35, 69.32, 45.39, 35.23, 33.69, 24.46, 20.85. Mass spectrometry (ESI-MS, m/z): $[M + H]^+$ calcd for ($C_{24}H_{21}N_3SBr$), 462.0640; found, 462.0638.

Synthesis of IBT. A mixture of **IB** (700 mg, 1.51 mmol), 5-formylthiophen-2-yl-2-boronic acid (230 mg, 1.5 mmol), $Pd(PPh_3)_4$ (80 mg, 0.07 mmol), saturated K_2CO_3 aqueous solution (10 mL, 2 M), and THF (30 mL) was refluxed for 12 h under argon. After the solution cooled, water was added and the reaction mixture was extracted three times with CH_2Cl_2. The combined organic layer was washed with water and brine, dried over anhydrous Na_2SO_4, and evaporated under reduced pressure. The crude product was purified by column chromatography (CH_2Cl_2/petroleum ether = 1/1) on silica gel to yield the product as a deep red solid **IBT** (400 mg, 0.81 mmol, 54%). Melting point: 175.8−178.8 °C. ^{1}H NMR (400 MHz, $CDCl_3$, ppm): δ 9.97 (s, 1H, CHO), 8.21 (d, J = 4.0 Hz, 1H, Ph-H), 8.04 (d, J = 7.6 Hz, 1H, Ph-H), 7.85 (d, J = 4.0 Hz, 1H, Ph-H), 7.80 (s, 1H, Ph-H), 7.76 (dd, J_1 = 8.4 Hz, J_2 = 1.6 Hz, 1H, Ph-H), 7.71 (d, J = 7.6 Hz, 1H, Ph-H), 7.24 (s, 2H, Ph-H), 7.19 (d, J = 8.4 Hz, 2H, Ph-H), 7.02 (d, J = 8.0 Hz, 1H, Ph-H), 4.89 (m, 1H, N−CH−CH), 3.95 (t, 1H, N−CH−CH), 2.36 (s, 3H, −CH₃), 1.62−2.12 (m, 6 H, indoline-H). ^{13}C NMR (100 MHz, $CDCl_3$, ppm): δ 183.05, 153.95, 149.41, 148.96, 142.86, 139.85, 136.97, 135.58, 135.49, 132.00, 129.84, 129.16, 127.86,

127.42, 126.56, 125.62, 123.08, 120.53, 107.33, 69.32, 45.35, 35.25, 33.63, 24.43, 20.84. Mass spectrometry (ESI-MS, m/z): $[M + H]^+$ calcd for $C_{29}H_{24}N_3OS_2$, 494.1361; found, 494.1365.

Synthesis of IBTM. The Suzuki reaction of **IB** (300 mg, 0.65 mmol) with 5-methylthiophen-2-yl-2-boronic acid (184.6 mg, 1.3 mmol) using $Pd(PPh_3)_4$ (80 mg, 0.07 mmol) as a catalyst in a THF/2 M K_2CO_3 aqueous solution (30 mL/10 mL) was carried out in a similar manner to that for **IBT**. The crude product was purified by column chromatography (CH_2Cl_2/petroleum ether = 1/5) to yield the **IBTM** as a red solid (250 mg, 0.52 mmol, 80%). Melting point: 164.2−168.0 °C. ^{1}H NMR (400 MHz, $CDCl_3$, ppm): δ 7.88 (d, J = 3.6 Hz, 1H, Ph-H), 7.81 (d, J = 7.6 Hz, 1H, Ph-H), 7.75 (s, 1H, Ph-H), 7.70 (dd, J = 8.4 Hz, 1H, Ph-H), 7.63 (d, J = 7.6 Hz, 1H, Ph-H), 7.24 (d, J = 9.2 Hz, 2H, Ph-H), 7.17 (d, J = 8.4 Hz, 2H, Ph-H), 7.02 (d, J = 8.4 Hz, 1H, Ph-H), 6.86 (dd, J = 3.6 Hz, 1H, Ph-H), 4.85 (t, 1H, N−CH−CH), 3.93 (q, 1H, N−CH−CH), 2.58 (m, 3H, −CH₃), 2.34 (s, 3H, −CH₃), 1.59−2.09 (m, 6H, indoline-H). ^{13}C NMR (100 MHz, $CDCl_3$, ppm): δ 154.12, 152.93, 148.31, 141.09, 140.18, 137.45, 135.30, 132.86, 131.58, 129.78, 128.71, 127.26, 127.07, 126.24, 125.54, 125.47, 125.08, 120.22, 107.42, 69.25, 45.43, 35.17, 33.73, 24.46, 20.81, 15.48. Mass spectrometry (ESI-MS, m/z): $[M + H]^+$ calcd for $C_{29}H_{26}N_3S_2$, 480.1568; found, 480.1562.

■ ASSOCIATED CONTENT

Ⓢ Supporting Information

Detailed ^{1}H NMR, ^{13}C NMR, ESI mass spectra, and properties of **IB**, **IBT**, and **IBTM**. This material is available free of charge via the Internet at http://pubs.acs.org.

■ AUTHOR INFORMATION

Corresponding Authors
*Z. Guo. E-mail: guozq@ecust.edu.cn.
*W. Zhu. E-mail: whzhu@ecust.edu.cn. Fax: (+86) 21-6425-2758.

Notes
The authors declare no competing financial interest.

■ ACKNOWLEDGMENTS

■ REFERENCES

(1) Rathore, R.; Abdelwahed, S. H.; Guzei, I. A. J. Am. Chem. Soc. **2004**, 126, 13582−13583.
(2) Mas−Torrent, M.; Crivillers, N.; Rovira, C.; Veciana, J. Chem. Rev. **2011**, 112, 2506−2527.
(3) Hicks, R. G. Org. Biomol. Chem. **2007**, 5, 1321−1338.
(4) Nishinaga, T.; Komatsu, K. Org. Biomol. Chem. **2005**, 3, 561−569.
(5) Park, J. S.; Karnas, E.; Ohkubo, K.; Chen, P.; Kadish, K. M.; Fukuzumi, S.; Bielawski, C. W.; Hudnall, T. W.; Lynch, V. M.; Sessler, J. L. Science **2010**, 329, 1324−1327.
(6) Fukuzumi, S.; Ohkubo, K.; D'Souza, F.; Sessler, J. L. Chem. Commun. **2012**, 48, 9801−9815.
(7) Pan, X. B.; Chen, X. Y.; Li, T.; Li, Y. Z.; Wang, X. P. J. Am. Chem. Soc. **2013**, 135, 3414−3417.
(8) Sreenath, K.; Suneesh, C. V.; Ratheesh Kumar, V. K.; Gopidas, K. R. J. Org. Chem. **2008**, 73, 3245−3251.
(9) Sreenath, K.; Suneesh, C. V.; Gopidas, K. R.; Flowers, R. A. J. Phys. Chem. A **2009**, 113, 6477−6483.

(10) Sumalekshmy, S.; Gopidas, K. R. *Chem. Phys. Lett.* **2005**, *413*, 294−299.

(11) Connelly, N. G.; Geiger, W. E. *Chem. Rev.* **1996**, *96*, 877−910.

(12) Ajayakumar, M. R.; Asthana, D.; Mukhopadhyay, P. *Org. Lett.* **2012**, *14*, 4822−4825.

(13) Jung, J. Y.; Kang, M.; Chun, J.; Lee, J.; Kim, J.; Kim, J.; Kim, Y.; Kim, S.; Lee, C.; Yoon, J. *Chem. Commun.* **2013**, *49*, 176−178.

(14) Chang, C.; Yueh, H.; Chen, C. *Org. Lett.* **2011**, *13*, 2702−2705.

(15) Sanna, E.; Martínez, L.; Rotger, C.; Blasco, S.; González, J.; García−España, E.; Costa, A. *Org. Lett.* **2010**, *12*, 3840−3843.

(16) Kar, C.; Adhikari, M. D.; Ramesh, A.; Das, G. *Inorg. Chem.* **2013**, *52*, 743−752.

(17) Dodani, S. C.; Leary, S. C.; Cobine, P. A.; Winge, D. R.; Chang, C. J. *J. Am. Chem. Soc.* **2011**, *133*, 8606−8616.

(18) Zou, Q.; Li, X.; Zhang, J. J.; Zhou, J.; Sun, B. B.; Tian, H. *Chem. Commun.* **2012**, *48*, 2095−2097.

(19) You, Y.; Han, Y.; Lee, Y.; Park, S. Y.; Nam, W.; Lippard, S. J. *J. Am. Chem. Soc.* **2011**, *133*, 11488−11491.

(20) Li, N.; Yu, X.; Tong, A. J. *Chem. Commun.* **2010**, *46*, 3363−3365.

(21) Sheng, R. L.; Wang, P. F.; Gao, Y. H.; Wu, Y.; Liu, W. M.; Ma, J. J.; Li, H. P.; Wu, S. K. *Org. Lett.* **2008**, *10*, 5015−5018.

(22) Wang, H. H.; Xue, L.; Fang, Z. J.; Li, G. P.; Jiang, H. *New J. Chem.* **2010**, *34*, 1239−1242.

(23) Kumar, M.; Kumar, N.; Bhalla, V.; Sharma, P. R.; Kaur, T. *Org. Lett.* **2011**, *14*, 406−409.

(24) Yuan, L.; Lin, W. Y.; Zheng, K. B.; He, L.; Huang, W. *Chem. Soc. Rev.* **2013**, *42*, 622−661.

(25) Sun, W.; Fan, J. L.; Hu, C.; Cao, J. F.; Zhang, H.; Xiong, X. Q.; Wang, J. Y.; Cui, S.; Sun, S. G.; Peng, X. J. *Chem. Commun.* **2013**, *49*, 3890−3892.

(26) Kim, H. N.; Ren, W. X.; Kim, J. S.; Yoon, J. *Chem. Soc. Rev.* **2012**, *41*, 3210−3244.

(27) Chen, Y.; Jiang, J. *Org. Biomol. Chem.* **2012**, *10*, 4782−4787.

(28) Yin, S.; Leen, V.; Snick, S. V.; Boens, N.; Dehaen, W. *Chem. Commun.* **2010**, *46*, 6329−6331.

(29) Huang, L.; Chen, F. J.; Xi, P. X.; Xie, G. Q.; Li, Z. P.; Shi, Y. J.; Xu, M.; Liu, H. Y.; Ma, Z. R.; Bai, D. C.; Zeng, Z. Z. *Dyes Pigm.* **2011**, *90*, 265−268.

(30) Que, E. L.; Domaille, D. W.; Chang, C. J. *Chem. Rev.* **2008**, *108*, 1517−1549.

(31) Finkel, T.; Serrano, M.; Blasco, M. A. *Nature* **2007**, *448*, 767−774.

(32) Millhauser, G. L. *Acc. Chem. Res.* **2004**, *37*, 79−85.

(33) Veale, E. B.; Kitchen, J. A.; Gunnlaugsson, T. *Supramol. Chem.* **2013**, *25*, 101−108.

(34) Upadhyay, K. K.; Kumar, A.; Zhao, J.; Mishra, R. K. *Talanta* **2010**, *81*, 714−721.

(35) Shi, L.; Li, Y.; Liu, Z.; James, T. D.; Long, Y. *Talanta* **2012**, *100*, 401−404.

(36) Ito, S.; Zakeeruddin, S. M.; Humphry−Baker, R.; Liska, P.; Charvet, R.; Comte, P.; Nazeeruddin, M. K.; Péchy, P.; Takata, M.; Miura, H.; Uchida, S.; Grätzel, M. *Adv. Mater.* **2006**, *18*, 1202−1205.

(37) Zhu, W. H.; Wu, Y. Z.; Wang, S. T.; Li, W. Q.; Li, X.; Chen, J.; Wang, Z. S.; Tian, H. *Adv. Funct. Mater.* **2011**, *21*, 756−763.

(38) Wu, Y. Z.; Zhu, W. H. *Chem. Soc. Rev.* **2013**, *42*, 2039−2058.

(39) Li, W. Q.; Wu, Y. Z.; Zhang, Q.; Tian, H.; Zhu, W. H. *ACS Appl. Mater. Interfaces* **2012**, *4*, 1822−1830.

(40) Pei, K.; Wu, Y. Z.; Islam, A.; Zhang, Q.; Han, L. Y.; Tian, H.; Zhu, W. H. *ACS Appl. Mater. Interfaces* **2013**, *5*, 4986−4995.

(41) Liu, B.; Zhu, W. H.; Zhang, Q.; Wu, W. J.; Xu, M.; Ning, Z. J.; Xie, Y. S.; Tian, H. *Chem. Commun.* **2009**, *46*, 1766−1768.

(42) Sreenath, K.; Thomas, T. G.; Gopidas, K. R. *Org. Lett.* **2011**, *13*, 1134−1137.

(43) Frisch, M. J.; Trucks, G. W.; Schlegel, H. B.; Scuseria, G. E.; Robb, M. A.; Cheeseman, J. R.; Scalmani, G.; Barone, V.; Mennucci, B.; Petersson, G. A.; Nakatsuji, H.; Caricato, M.; Li, X.; Hratchian, H. P.; Izmaylov, A. F.; Bloino, J.; Zheng, G.; Sonnenberg, J. L.; Hada, M.; Ehara, M.; Toyota, K.; Fukuda, R.; Hasegawa, J.; Ishida, M.; Nakajima, T.; Honda, Y.; Kitao, O.; Nakai, H.; Vreven, T.; Montgomery, J. A.; Peralta, J. J. E.; Ogliaro, F.; Bearpark, M.; Heyd, J. J.; Brothers, E.; Kudin, K. N.; Staroverov, V. N.; Kobayashi, R.; Normand, J.; Raghavachari, K.; Rendell, A.; Burant, J. C.; Iyengar, S. S.; Tomasi, J.; Cossi, M.; Rega, N.; Millam, J. M.; Klene, M.; Knox, J. E.; Cross, J. B.; Bakken, V.; Adamo, C.; Jaramillo, J.; Gomperts, R.; Stratmann, R. E.; Yazyev, O.; Austin, A. J.; Cammi, R.; Pomelli, C.; Ochterski, J. W.; Martin, R. L.; Morokuma, K.; Zakrzewski, V. G.; Voth, G. A.; Salvador, P.; Dannenberg, J. J.; Dapprich, S.; Daniels, A. D.; Farkas, O.; Foresman, J. B.; Ortiz, J. V.; Cioslowski, J.; Fox, D. J. *Gaussian 09*, Revision A.02; Gaussian, Inc.: Wallingford, CT, 2009.

(44) Kamau, P.; Jordan, R. B. *Inorg. Chem.* **2001**, *40*, 3879−3883.

12220

dx.doi.org/10.1021/am404491f | *ACS Appl. Mater. Interfaces* 2013, 5, 12215−12220